Magnetic Field Calculation and Characteristic Analysis on Double-acting VCM for Intelligent Vehicle Suspension

Liguo Miao[1] ,Feng Sun[1],Wei Wei[1],Zhiyu Zhao[1],Qiang Li[1],Fangchao Xu[1],Fei Pan[1],Xiaoyou Zhang[2]

[1]Shenyang University of Technology, No.111, Shenliao West Road, Economic and Technological Development Area, Shenyang, China, sunfeng@sut.edu.cn

[2]Nippon Institute of Technology, Department of Mechanical Engineering, Japan, zhang@nit.ac.jp

***Abstract*—For the shortcomings of MacPherson independent suspension vehicle, such as brake nod obvious, large roll, poor stability and the vibration energy dissipation of the suspension system, A kind of magnetic field structure of VCM (Voice Coil Motor) combined with active control and energy recycle is proposed. In this paper, a 3D model of the VCM is designed, and introduced the structure in detail, Secondly, the mathematical model of the VCM quasiparallel magnetic field is established, the 3D model is analyzed, aiming at the maximum flux density and limited by the size of the motor. Based on the calculation of magnetic field, the influence of each parameter on the flux density of the motor is analyzed, and the prototype is designed. The results show that magnetic field model of the VCM is verified. Deviation within the acceptable range exist between the experimental value and the theoretical value, Analyzed influencing factors of the VCM characteristics, the VCM prototype has ideal output force characteristics. It has provided an important theoretical foundation for design and development of such suspension.**

I. INTRODUCTION

Suspension is one of the most important mechanisms of automobile chassis, whose function is to transfer the force or torque between the wheel and frame, and at the same time dampen vibration from the uneven road to the body of vehicle in order to ensure that the vehicle can run smoothly[1-4]. In this process, the mechanical energy of vehicle vibration is converted into heat and emanated into the atmosphere, it's a loss of energy. In the design of the traditional passive suspension due to the determined structural parameters, the selection of stiffness and damping parameters can only be solved by using a compromise method, which can not take into account the driving safety and ride comfort requirements of the vehicle. In recent years, with the improvement of various hardware facilities, vehicle have also been greatly accelerate. Therefore, it is necessary to promote active / semi-active suspension with higher performance[5].

The semi-active suspension can adjust the damping of shock absorber by consuming less energy. Solenoid valve and magnetorheology are two main ways of adjustment. Solenoid valve was used earlier, but its structure has some problems such as operation noise, hysteresis and instability. The Magnetorheological shock absorber has compact structure and rapid response, but its problems such as durability and adaptability to the environment still need to be solved[6-10]. Active suspension get the best performance between the riding comfort and handling safety of automobiles on different roads by active control. At present, high pressure cylinder actuators are mostly used. The energy recycle suspension was proposed by some scholars, which is a kind of active control suspension. The energy recycle suspension can not only improve the motion performance of the vehicle, but also reduce energy loss by recover vibration energy[11-12]. The energy recycle suspension is mainly divided into mechanical and electro-hydraulic structures, and it is difficult to popularize and apply on a large scale because the new structure is used instead of the traditional damping structure, and the damping characteristic of the original suspension is changed.

In this paper, a new intelligent suspension system based on McPherson independent suspension is proposed. As shown in fig. 1. The system has two modes: active control mode and energy recycle mode. Based on the traditional Macpherson suspension structure, the functional characteristics of the VCM is accumulated, the change of original suspension characteristics is avoided, and the dual action of active control and energy feed can be achieved. Firstly, the VCM structure is proposed, structure and working principle is introduced. Secondly, magnetic field mathematical model of the VCM is established. The 3D model and the influence of VCM design parameters on the flux density of the motor is analyzed. Finally, a prototype is builted and the magnetic field and output force characteristics of the VCM is tested.

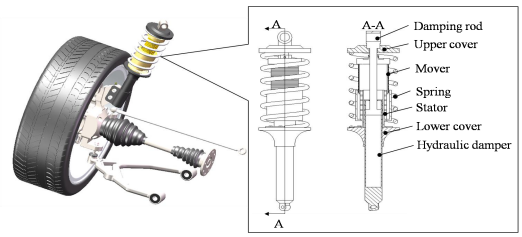

Fig. 1 Intelligent suspension system

II. STRUCTURE AND PRINCIPLE OF THE PROPOSED SUSPENSION

A Structure of the proposed suspension

Taking Macpherson suspension as an example, the designed suspension structure is shown in fig. 1. The VCM was designed in the gap between the shock absorber and spring, the motion of the VCM is connected to the upper tray

of the shock absorber, and the stator of the VCM is connected to the lower tray of the shock absorber. The stroke of the stator is less than the maximum dynamic deflection of the suspension to avoid collsion.

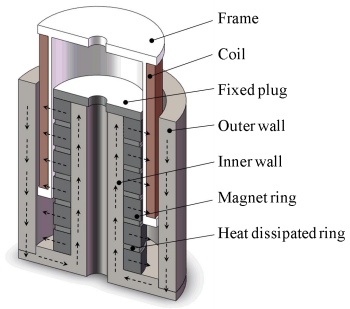

Fig. 2 Structure of the stator

The VCM is consists of two major parts: mover and stator, the structure is shown in fig. 2. The voice coil is mover which consists of a coil and a bobbin, and moves along the axis of the VCM. The stator consists of the magnetic yok, six magnet rings, heat dissipated rings and fixed plug. The ring magnet and the heat dissipated ring are arranged alternately in the axial direction of the inner yoke. Heat dissipated ring accelerates heat flow of magnetic rings and avoid overheating, The top of the magnetic ring is a plug, which can fix the magnet and reduce magnetic leakage. Each magnet ring is composed of eight same pieces, the magnet rings are magnetized the inside as S pole and the outside as N pole. In this application. When permanent magnetic material is used in high temperature or exquisite mechanical vibration, it may produce irreversible demagnetization. In order to prevent this situation, The structure of alternating arrangement of magnetic and aluminum ring is designed to ensure VCM heat dissipation.

B Principle of the proposed suspension

The energy flow of the suspension system is shown in fig. 3. On the one hand, the mechanical energy of vibration is converted into electric energy stored in batteries and reduced vehicle energy consumption. On the other hand, the damping force can be provided by controlling the linear motor to suppress the vibration of the body caused by the excitation of uneven road surface, and which can improve the ride comfort and handling stability of the vehicle.

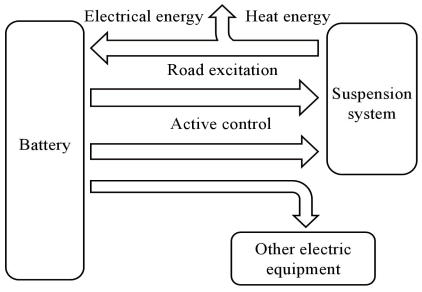

Fig. 3 Energy flow of suspension system

As shown in Fig. 4, the structural design of the active suspension can be explained by the 1/4 body model. It consists of the body, the wheel, the suspension spring, the VCM actuator, the processor and the electric storage medium (the energy storage circuit, the vehicle power supply), the displacement sensor, the acceleration sensor. Among them, suspension springs, VCM actuators and displacement sensors are installed in parallel between the vehicle body and wheel.

A quasi-parallel magnetic field is produced by a magnetic ring under the action of a yoke, The quasi-parallel magnetic field is perpendicular to the surface of the magnetic ring, and the direction is from the N level of the magnetic ring through the air gap, the outer yoke, and the inner yoke to the S level. The cycle mode is shown in Fig. 2. According to the ampere force theorem, when the coil is electrified, an axial electromagnetic will is produced force by electrified coil, which makes the ring movement. The speed and direction of the voice coil movement are related to the current size and direction. Working principle of intelligent vehicle suspension is shown in fig. 4. The signal measured by displacement sensor and acceleration sensor is inputted into processor, After the logic algorithm calculation, the VCM actuator is controlled in real time by battery, onboard circuit. The automobile spring is compressed or springback rapidly when vehicle under normal conditions. The coil cuts magnetic induction line and generates current. The recovered current is converted into direct current by rectifier circuit and stored in the battery, which can save energy. when vehicle was on the bumpy road, The damping force of vehicle can be indirectly affected by the active control VCM device and the movement performance of vehicle is improved.

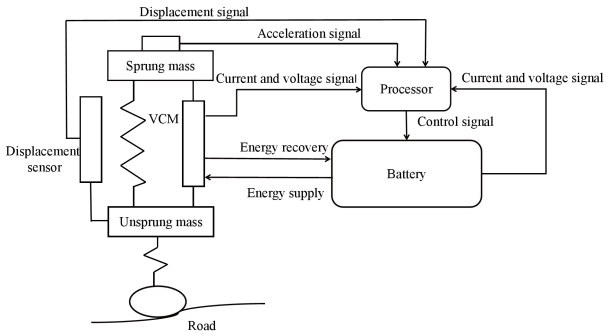

Fig. 4 Working principle of intelligent vehicle suspension

III. MODEL AND THEORETICAL ANALYSIS OF MAGNETIC FIELD

In VCM, the air gap magnetic field is one of the main factors to improve the performance of the motor. The actuator thrust size and generator energy recovery efficiency are determined by the magnetic flux density in the air gap. The air gap magnetic density model was established and the characteristics of the magnetic field were theoretically analyzed.

A magnetic flux density model of single magnetic ring

In order to analyze quasi-parallel magnetic field in the air gap of the VCM. Magnetic flux density model of single magnetic ring was established. O is origin of coordinate and locates in the center of the model. The magnetic field in y direction was calculateed and x direction is ignored. As shown in Fig. 5. According to analytical theory of Halbach

permanent magnetic array[16]. When the positive direction of the magnet field is +*y* direction, the spatial magnetic field can be equivalent to the magnetic field generated by surface currents 1 and 2.

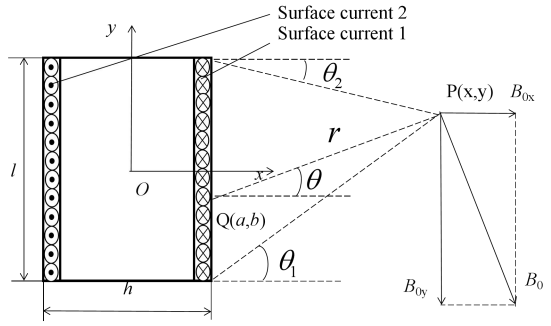

Fig 5 Schematic Diagram of the Magnetic Field of Single Magnet Ring

As shown in fig. 5. Q is at any point line current element of the surface current 1. B_0 is magnetic field which is producted by Q at point P

$$B_{oy} = -B_0 \cos\theta \tag{1}$$

where，

$$B_0 = \frac{\mu_0 k_v}{2\pi r};\theta = \arcsin(\frac{y-b}{r}) \tag{2}$$

Where

μ_0——Permeability of vacuum(H/m)

k_v——Current line density

R——The distance of Q point to space point P

h——cross section width of magnet ring

l——cross section length of magnet ring

θ——Angle between the line of point Q and point P and the horizontal line

The magnetic flux density B_{y11} generated by the surface currents1 can be expressed as (3)

$$\begin{aligned} B_{y11} &= -\int_{\theta_1}^{\theta_2} \frac{u_0 k_v}{2\pi r}\cos\theta db \\ &= \frac{u_0 k_v}{2\pi}[\arctan(\frac{y+l/2}{x+h/2}) - \arctan(y=\frac{y-l/2}{x+h/2})] \end{aligned} \tag{3}$$

where，

$$\begin{aligned} r &= \frac{x-h/2}{\cos\theta} & db &= -\frac{x-h/2}{(\cos\theta)^2}d\theta \\ \theta_1 &= \arctan(\frac{y+l/2}{x-h/2}) & \theta_2 &= \arctan(\frac{y-l/2}{x-h/2}) \end{aligned} \tag{4}$$

The magnetic flux density B_{y12} generated by the surface currents2 can be expressed as (5).

$$\begin{aligned} B_{y12} &= -\int_{\theta_1'}^{\theta_2'} \frac{\mu_0 k_v}{2\pi r}\cos\theta db \\ &= \frac{\mu_0 k_v}{2\pi}[\arctan(\frac{y+l/2}{x+h/2}) - \arctan(\frac{y-l/2}{x+h/2})] \end{aligned} \tag{5}$$

Where

θ_1——Angle between starting point of current and horizontal direction

θ_2——Angle between end point of current and horizontal direction

B Magnetic flux density model of the VCM's stator

A mathematical model of the magnetic flux density array in the y direction air gap is established.

$$B_y = \sum_{i=1}^{6} B_{yj1} + \sum_{i=1}^{6} B_{yj2} \tag{6}$$

$$B_{yj} = B_{yj1} + B_{yj2}$$

$$\begin{aligned} B_{yj1} &= \frac{\mu_0 k_v}{2\pi}\arctan(\frac{y-l/2}{x-(j-1)\cdot(h+s)-h/2}) \\ &- \frac{\mu_0 k_v}{2\pi}\arctan(\frac{y+l/2}{x-(j-1)\cdot(h+s)-h/2}) \end{aligned} \tag{7}$$

$$\begin{aligned} B_{yj2} &= \frac{\mu_0 k_v}{2\pi}\arctan(\frac{y+l/2}{x-(j-1)\cdot(h+s)+h/2}) \\ &- \frac{\mu_0 k_v}{2\pi}\arctan(\frac{y-l/2}{x-(j-1)\cdot(h+s)+h/2}) \end{aligned} \tag{8}$$

IV. MAGNETIC FIELD ANALYSIS

A FEM analysis model

The FEM characteristic analysis of the VCM 3D model is done by ansoft, In the FEM model, the remanence B_r of the permanent magnet is 1.18T, and the coercivity is -880000A/m. The results of FEM is shown in Fig. 6. The permanent magnetic flux loop in the stator is closed, and the magnetic flux leakage is less. The magnetic flux is nearly parallel in the air gap, and its distribution is relative in the air gap except the two ends. This proves that when it moves in the air gap, the coil moves though cutting the parallel magnetic flux.

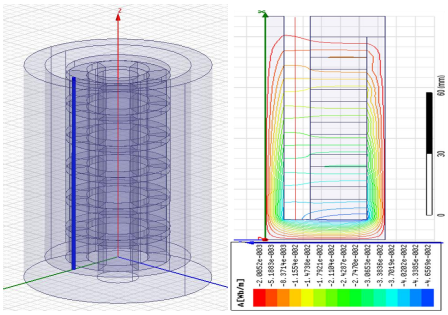

（a） （b）

Fig 6 FEM analysis on magnetic field of the VCM stator. (a) Finite element model (b) Simulation results.

B Analysis of design parameters on the performance of VCM

The force of the motor winding

$$F = BIL \tag{9}$$

The F is the magnetic force to which the winding is subjected, B is magnetic induction intensity of air gap, I is voice coil current, L is coil length in magnetic field.

Formula (9) shown that the thrust of the motor is proportional to the intensity of the magnetic field when the current I and the coil length L are fixed. In order to get the optimal motor performance. The influence of different design parameters on the performance of the VCM is quantitatively simulated and analyzed. The outer diameter of stator is less than 100mm and the height is less than 110mm. Based on the

middle position of the air gap shown in Fig. 6, magnetic flux density simulation is analyzed.

Structural parameters affecting the performance of the VCM include magnetic steel thickness, magnet height, air gap distance, outer yoke thickness, and heat ring height. Based on the calculation of magnetic field, the influence of each parameter on the flux density of the motor is analyzed.

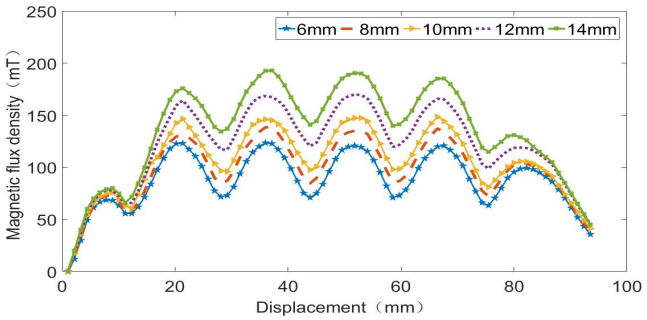

Fig 7 Influence of different magnetic stiffness on air gap magnetic density

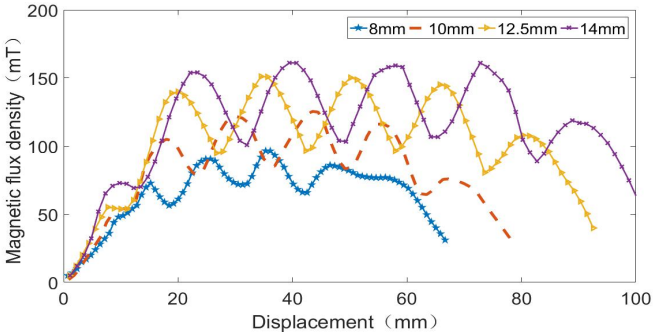

Fig 8 Influence of different height of magnetic steel on air gap magnetic density

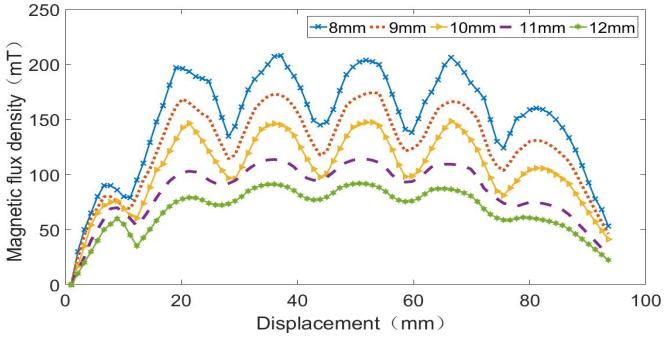

Fig 9 Influence of different air gap on air gap magnetic density

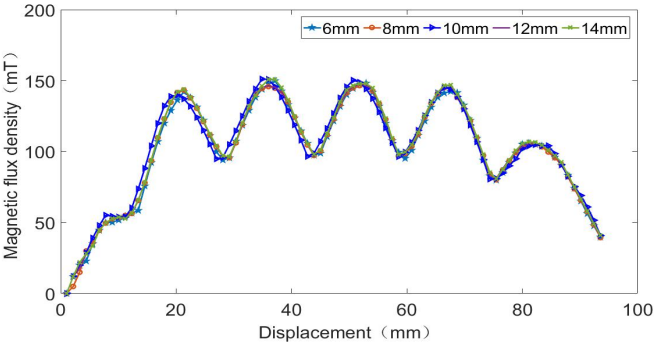

Fig 10 Influence of different thickness of outer magnetic yoke on air gap magnetic density

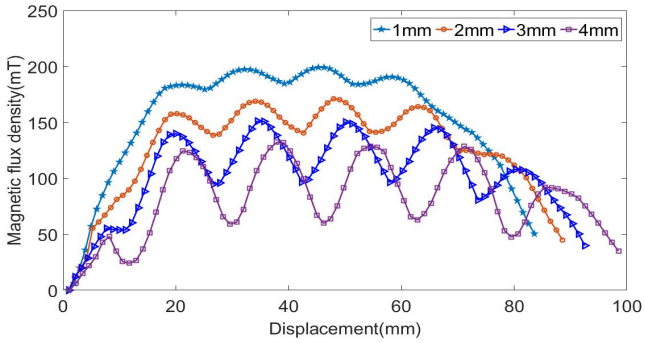

Fig 11 Influence of different height of heat dissipation ring on air gap magnetic density

It can be seen that the height and thickness of magnetic steel are directly proportional to the magnetic induction intensity when the other parameters are fixed. On the contrary, the larger the air gap spacing, the smaller the relative air gap flux density. The change of air gap density gradually decreases when the thickness reaches a certain level. The thickness of outer yoke has little effect on air gap flux density because the external magnetic yoke is thinner, the magnetic flux leakage is more and compared with 6mm, 14mm increases only 0.03%. The larger the cooling ring and the volume, the smaller the relative magnetic density, but the small cooling ring will lead to heat dissipation slowing down, demagnetized and the effective length reduction in the axial magnetic field of the VCM.

The real car test was not carried out due to the limitation of vehicle and experimental conditions, According to the simulation results and processing conditions. A small device is designed to verify characteristics of the VCM, The specific parameters of the prototype design are shown in Table 1.

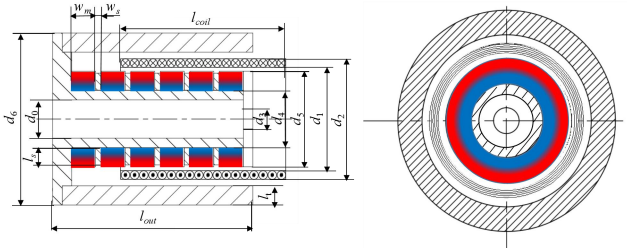

Fig 12 Sectional view of the VCM

TABΛE I

TABLE I. MAJOR PARAMETERS TABLE OF VCM

Symbol	Parameters	Values
d_0	Diameter of the shaft hole in inner wall / mm	19
d_1	Inside diameter of the coil / mm	56
d_2	Outside diameter of the coil / mm	22
d_3	Diameter of the hole in fixed plug / mm	12
d_4	Inside diameter of the magnet ring / mm	30
d_5	Outside diameter of the magnet ring / mm	50
d_6	Diameter of the stator / mm	90
l_s	Length of the heat dissipated ring / mm	10
w_m	Width of the magnet ring / mm	12.5
w_s	Width of the heat dissipated ring / mm	3
l_{coil}	Length of the coil in the axial direction / mm	90
l_t	Thickness of the outer wall of VCM / mm	10
l_{out}	Length of the stator in axial direction / mm	105

V. EXPERIMENTAL VERIFICATION

A Experimental devices

In order to analyze magnetic field and output force characteristics of the intelligent suspension system, experimental device is set up to verify and analyze its characteristics. The experimental device of the VCM is shown in the Fig. 4. The VCM prototype are constructed with the stator and mover, its inner wall and outer wall of stator is made of the electrician soft iron, its magnet ring is N35H, the number of its coil's turns is 3170, the diameter of lacquered wire is 0.38mm, and its total resistance is 62 Ω. The frame's material is epoxy rods. The weight of the stator and coil are respectively4.045kg and 0.594kg.

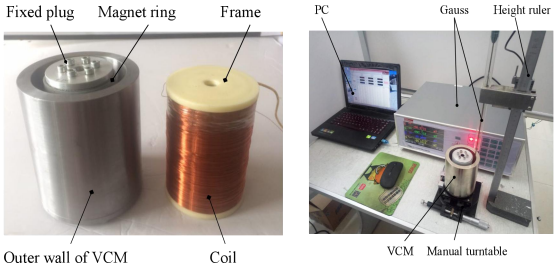

(a) (b)

Fig 15 The experimental device of the VCM.（a）Prototype of the VCM （b）The experimengal device of magnetic field analysis

B Experimental analysis

In the prototype, each magnetic ring is composed of eight identical components, and the annular magnetic steel is composed of a parallel magnetized tile magnetic steel, which will have a certain error effect on the experimental results. First, the ring error of the prototype magnetic steel is analyzed and the data acquisition position is shown in Fig. 14(a). The measured position is 50 mm from the top plug and 5 mm from the inner wall of the yoke. The simulation position is the same as the measuring position. The data are recorded every 5 degrees and the average value is gained by multiple measure. The experimental and simulation results are shown in Fig. 14(b). The polar angle represents the angle of air gap in the stator, the polar radius represents the magnetic flux intensity in the air gap of stator. The results show that the peak value and periods of the experimentis data is accordance with simulation. The phase has a 3° deviation because the measuring starting position is different from position of the simulation data acquisition. The maximum B of simulation is 172.31mT, the minimum B is 118.16mT, the maximum B of experiment is 170.19mT, and the minimum B of expe-riment is 109.96mT.

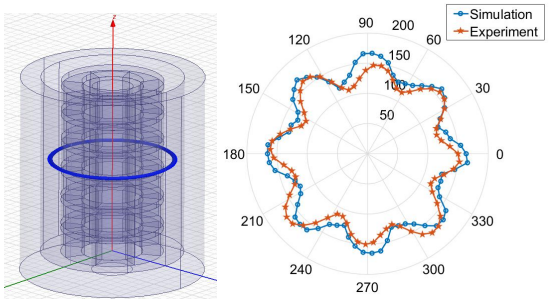

(a) (b)

Fig 14 Diagram of the magnetic field analysis (a) Finite element model, (b) Experimental results.

Secondly, the magnetic field model and finite element simulation are tested and verified. The experimental equipment is shown in fig. 13(b), and consists of PC, gauss meter, VCM, and bench, measurement position is shown in the Fig. 6(a). The distance between gauss meter and inner wall of yoke is 5 cm. Experimental data is recorded once per 2mm from top to bottom. The measureing position is the same as FEM position. The magnetic field curve is given by bring parameter of the VCM into the magnetic field mathematical model, result is shown in figure 15.

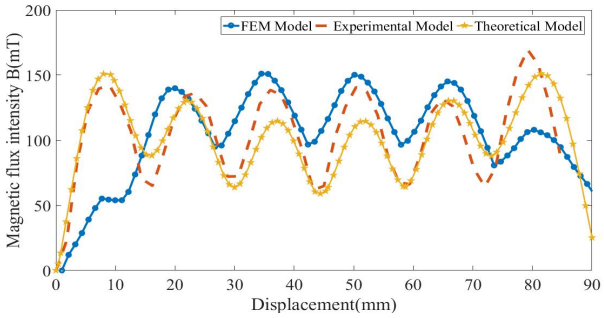

Fig. 15 Comparative results of magnetic flux density

The comparative results of magnetic flux density are shown in Fig. 15. The trend of the theoretical calculation, FEM analysis and experimental result is approximately similar. Since theoretical calculations ignores the outer wall of motor and the fixed plug, the value of the flux density on theoretical calculation on both sides is higher than the results of the FEM simulation curve. The average values of magnetic flux density in experiment, theory and simulation are respectively 104.5mT, 98.6mT and 104.7mT, The error is mainly caused by the measurement error of magnet specification, manual measurement error, probe size of Tesla and the influence of uneven magnetic field distribution of magnet boundary. The experiment shows that the sixth magnetic field is larger because of the magnetization error.

Finally,as shown in Fig. 16, the output characteristics of the VCM are tested. The experimental equipments are composed of bench, force sensor, ammeter, VCM, monitor, DSP (dSPACE 1103), power amplifier, and PC. The spec-ific parameters of the force sensor are shown as follows: measuring range is 0-300N, measuring precision is ±(2.0%+5), and resolution is 0.01N.

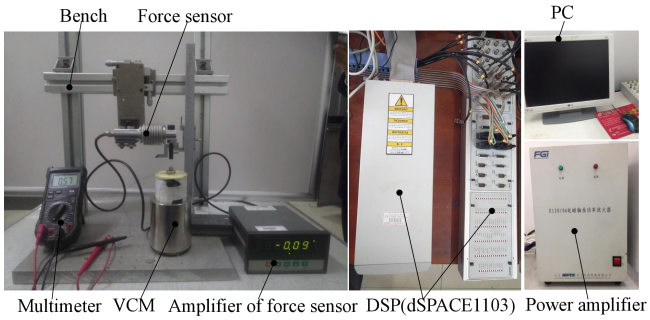

Fig 16 Experimental equipments of active control mode

The experiment was divided into two groups to measure. The relation between current and output force, displacement and output force. 0V-1.3V are as input voltage parameters, the voltage signal of DSP (dSPAC-E1103)is turned to current signal of power amplifier and the current signal drives the VCM. The stator is fixed to the underboard of the bench and force sensor is fixed on bench. The measures head of the force sensor and the upper end of the coil are fixed together. The coils are aligned with the stator axis to reduce friction in motion. The experiment of the relation between the current and the output force shows the output force of the VCM under different currents. As the diameter of the enameled wire is very thin, the maximum current is 0.9A (0.05A is as an interval) to protect the coil from overheating and burning. The relation between the displacement and the output force is measured, current is constant and the output force is measured at intervals of 3 mm. The experimental currents are respectively 0.4A, 0.5A and 0.6A.

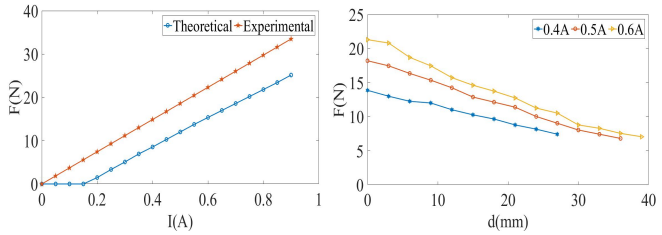

Fig 17 The curves of the VCM characteristics: (a) The relationship of the current and output force, (b) The relationship of the displacement and output force.

The relation between current and output force is shown in fig. 17(a). When the current is 0.9A, the maximum value of the theoretical curve is 33.84N because the weight 5.84N of the bracket and the coil is ignored. The point in 0.15A represents that the VCM completely overcomes the weight of the coil to produce output force, The current is linear with the output force when the current range is 0.15~0.9A, and the current coefficient K is 33.28. The relationship of the displacement and output force is shown in the Fig. 17(b), the displacement *d* represents the length of the coil in the outside of the stator. The three curves are the values of the output force when current 0.4A, 0.5A, and 0.6A is applied separately, and approximately linear. Their displacement coefficients from top to bottom are -0.37, -0.31, and -0.23.

VI. Conclusion

An kind of double-acting VCM for intelligent vehicle suspension is designed. Based on the calculation of magnetic field, the magnetic field distribution in VCM air gap space and the influence of design parameters on the performance of the VCM are analyzed by FEM software. The structural parameters affecting the characteristics of the VCM include the thickness of magnetic steel, the thickness of voice coil, the thickness of external yoke, the distance of air gap to the height of heat dissipation ring. Among them, the thickness of magnetic steel and the air gap distance are the most important ones. By comparing the results of the measurement, calculated and the simulation, it is found that the established analytical expression can well reflect change regulation of VCM magnetic field in air gap. The experimental value and the theoretical value have a deviation in the acceptable range, and the analytical expression is verified. The test results of the output force characteristic of the VCM shows that the VCM designed in this paper has larger output force. The "current displacement" and the "current output force" curve are well linear, and the design is meets actual requirements.

Acknowledgements

This research is supported by the following projects of Liaoning Province (No. LR2017036, No. 20170520177, No. 2015-47).

References

[1] Zhang Yongchao, Zheng Xuechun, Yu Fan, et al. Theoretieal and Experimental Study on Eleetrieal Ener-Regenerative Suspension[J]. Automotive Engineering, 2008, 30(1):48-52.

[2] Wu Linlin, Shi Mingmin, Wang Ruochen, et al. Parameter Optimization of Hybrid Suspensionwith Linear Motor Based on PSO[J]. Journal of Chongqing University of Technology, 2016, 30(11):12-17.

[3] Kou farong, Liang Jin, Wei Dongdong, Wang Xing, Tian Lei. Research on a Parallel Type Semi-active Suspension Actuator[J]. Chinese Journal Of Mechanical Engineering, 2017,28(19):2318-2324.

[4] Chen Shuang, Zong Changfu, Liu Liguo, et al. Co-simulation on the Coordinated Control of Ride Comfort andHandling Stability of Vehicles with Active Suspension[J]. Automotive Engineering, 2012, 34(9):791-797.

[5] Cao Min, Liu Wei, Yu Fan. DeveloPment on Eleetormotor Aetuator for Aetive SusPension of Vehiele[J]. Journal Of Mechanical Engineering, 2008, 44(11):224-228.

[6] Metered H, Bonello P, Oyadiji S O. The experimental identification of magnetorheological dampers and evaluation of their controllers[J]. Mechanical Systems & Signal Processing, 2010, 24(4):976-994.

[7] Goncalves F D, Ahmadian M, Carlson J D. Investigating the magnetorheological effect at high flow velocities[J]. Smart Materials & Structures, 2005, 15(1):75.

[8] Spelta C, Previdi F, Savaresi S M, et al. Control of magnetorheological dampers for vibration reduction in a washing machine[J]. Mechatronics, 2009, 19(3):410-421.

[9] Peng Zhizhao, Zhang Jinqiu, Yue Jie, et al. Design and Analysis of Magnetorheological Damper Paralleling withConstant Throttling Orifices[J]. Journal of Mechanical Engineering, 2015, 51(8):172-177.

[10] Xing Jian, He Lidong, Wang Kai. Experimental study of active control techniques for single span rotor vibration reduction [J]. Chinese Journal of Scientific Instrument , 2013(s1):48-54.

[11] Zou Z, Cao J, Cao B, et al. Evaluation strategy of regenerative braking energy for supercapacitor vehicle[J]. Isa Transactions, 2015, 55:234.

[12] Chen S A, Li X, Zhao L J, et al. Development of a control method for an electromagnetic semi-active suspension reclaiming energy with varying charge voltage in steps[J]. International Journal of Automotive Technology, 2015, 16(5):765-773.

[13] Cao Min, Liu Wei, Yu Fan. DeveloPment on Eleetormotor Aetuator for Aetive SusPension of Vehiele[J]. Journal of Mechanical Engineering, 2008, 44(11):224 - 228.
[14] Yu Changmiao, Wang Weihua, Subhash, et al. Experiments and analysis of the dual-overruning clutches electro-mechanical regenerative damper prototype[J]. Journal of Jilin University, 2012, 42(2):292-297.
[15] Zhang Han, Guo Xuexun, Xu Lin, et al. Simulation and test for hydraulic electromagnetic energy-regenerative shock absorber[J]. Transactions of the CSAE, 2014, 30(2):38-46.
[16] Zhang Yin, Zhang Kunlun. Analytic calculation of the magnetic field created by Halbach permanent magnets array[J]. Journal of Magnetic Materials and Devices, 2014(1):1-4.